ARTICLE

ACS chemical biology

Ligand Switching in Cell-Permeable Peptides: Manipulation of the α-Integrin Signature Motif

Elise Bernard[†,#], Laavanya Parthasarathi[†,#], Min-Kyu Cho[‡], Kelly Aylward[†], Markus Raab[†], Heide Daxecker[†], Colm T. O'Dushlaine[§], Denis C. Shields[¶], Marc Devocelle[⊥], Tia Keyes[∥], Lynda Cosgrave[∥], Sarah O'Neill[†], Kenneth H. Mok[‡], and Niamh Moran*[,†]

[†]Molecular & Cellular Therapeutics (MCT), and [⊥]Centre for Synthesis and Chemical Biology, Royal College of Surgeons in Ireland, Dublin 2, Ireland, [‡]School of Biochemistry & Immunology, and [§]Department of Psychiatry, Trinity College Dublin, Dublin 2, Ireland, [¶]UCD Conway Institute, Dublin 4, Ireland, and [∥]School of Chemical Sciences, Dublin City University, Dublin 9, Ireland. #These authors contributed equally to this work.

ABSTRACT A synthetic cell-permeable peptide corresponding to the highly conserved α-integrin signature motif, Palmityl-K^{989}VGFFKR^{995} (Pal-FF), induces integrin activation and aggregation in human platelets. Systematic replacement of the F^{992}-F^{993} with amino acids of greater or lesser hydrophobicity to create Pal-KVGxxKR peptides demonstrate that hydrophobic amino acids (isoleucine, phenylalanine, tyrosine, tryptophan) are essential for agonist potency. In marked contrast, substitution with small and/or hydrophilic amino acids (glycine, alanine, serine) causes a switch in the biological activity resulting in inhibition of platelet aggregation, adhesion, ADP secretion, and thromboxane synthesis. These substituted, hydrophilic peptides are not true pharmacological antagonists, as they actively induce a phosphotyrosine signaling cascade in platelets. Singly substituted peptides (Pal-AF and Pal-FA) cause preferential retention of pro- or anti-thrombotic properties, respectively. Because the α-integrin signature motif is an established docking site for a number of diverse cytoplasmic proteins, we conclude that eliminating critical protein−protein interactions mediated through the hydrophobic amino acids, especially F^{993}, favors an anti-thrombotic pathway in platelets. Agents derived from the inhibitory peptides described in this study may represent a new therapeutic strategy for anti-platelet or anti-integrin drug development.

Integrins are a family of cell surface receptor molecules that are critical for cell adhesion in many important biological processes. The platelet integrin $\alpha_{IIb}\beta_3$ is perhaps the most studied of all integrins as it plays a major role in arterial hemostasis and thrombosis, and its platelet specificity has identified it as an ideal target for anti-platelet therapy in the treatment of thrombotic disease. However, the recent failure of the oral integrin $\alpha_{IIb}\beta_3$ antagonists to safely treat patients with cardiovascular disease has highlighted the need to better understand the complex intracellular signaling network that both permits and propagates integrin activation (*1, 2*). A better understanding of these processes may allow the development of better anti-platelet or anti-integrin agents.

The importance of the cytoplasmic domain of α_{IIb} in regulating the affinity of $\alpha_{IIb}\beta_3$ for its ligand has been established (*3, 4*). The highly conserved KVGFFKR α-integrin signature motif maintains the integrin in a default low-affinity state through a coordinated association with the integrin β_3 cytoplasmic tail (*3, 5–7*). In contrast, dissociation of the integrin α-β tails results in integrin activation (*4, 8, 9*). Moreover, deletion of the KVGFFKR regulatory region or introduction of mutations induces a constitutive activation of the integrin (*4, 10*). Thus, the α-integrin signature motif plays a critical role in regulating integrin function in the platelet.

In addition to its association with the β_3 tail, the KVGFFKR motif also acts as a recognition site for multiple intracellular proteins such as CIB1 (*11*), AUP-1 (*12*), PP1C (*13*), PP2A (*14*), ICln (*15*), RN181 (*16*), and TIM (*17*).

***Corresponding author,**
nmoran@rcsi.ie.

Received for review October 27, 2008 and accepted April 15, 2009.

Published online April 16, 2009

10.1021/cb8002623 CCC: $40.75

Thus the α_{IIb} cytoplasmic tail is emerging as a molecular scaffold for the coordination of interactions of cytoplasmic and cytoskeletal proteins in the regulation of downstream signaling to promote or modulate platelet responses. However, the mechanisms by which these interactions act to regulate integrin signaling in a dynamic cell system have yet to be fully elucidated. Therefore, understanding the role of the KVGFFKR motif of the α_{IIb} cytoplasmic tail is critical for understanding integrin activation and its control in platelets.

We have previously demonstrated, using cell-permeable synthetic KVGFFKR peptides, that this region both regulates integrin activation and independently initiates integrin signaling in platelets (*10, 18*). The critical role of the hydrophobic phenylalanine residues F^{992}-F^{993} of this motif was illustrated by Vinogradova (*19*) and Weljie (*20*) in their respective models of the structure of the cytoplasmic tails of the platelet integrin. Finally, mutation studies in which one or both of these residues is replaced with alanine induces constitutive ligand binding, demonstrating the role for F^{992}-F^{993} in the facilitated activation of the integrin (*21*). However, we have recently demonstrated that despite this activation of the integrin's capacity for ligand binding, replacing the hydrophobic phenylalanine residues also results in a disturbance in the capacity of the "activated" integrin to convey the correct signals within the cell in mutant CHOα_{IIb} F^{992}A,F^{993}A β_3 cells (*10*). Moreover, replacement of phenylalanine residues with the less hydrophobic alanine in cell-permeable peptides results in a loss of agonist potency in synthetic KVGAAKR peptide studies. Thus, the KVGFFKR motif coordinates both integrin activation and downstream signaling events including actin assembly. In this Article, we will explore the molecular requirements for this regulatory process.

We examine the effects of synthetic cell-permeable peptides in assays of platelet function and tyrosine phosphorylation as an index of platelet response. All data is quantified relative to a maximal response obtained in the presence of a thrombin-receptor activator. We observe that some peptides actively inhibit platelet responses to agonists. Studies to explore this unexpected result demonstrate that the inhibitor peptides are integrin-specific but are not true integrin antagonists, as they independently provoke a tyrosine phosphorylation response. Thus, they will be useful tools in dissecting the integrin-activated pathways in platelets. In this Article we will establish the chemical characteristics of pro-thrombotic and anti-thrombotic peptides in order to gain a better understanding of integrin signaling pathways in human platelets.

RESULTS AND DISCUSSION

Importance of F^{992}-F^{993} for Regulation of Integrin $\alpha_{IIb}\beta_3$. We have previously demonstrated that a cell-permeable, palmitylated KVGFFKR peptide (Pal-FF), corresponding to the regulatory motif of the major platelet α-integrin cytoplasmic domain, but not a related peptide Pal-KVGAAKR (Pal-AA), induces platelet activation (*10*). To explore the precise requirements for the hydrophobic phenylalanines on the function of the integrin regulatory motif, we used palmitylated substituted KVGxxKR peptides (Pal-XX) as follows: Pal-KVGFFKR (Pal-FF), Pal-KVGAAKR (Pal-AA), Pal-KVGIIKR (Pal-II), Pal-KVGYYKR (Pal-YY), Pal-KVGWWKR (Pal-WW), Pal-KVGGGKR (Pal-GG), and Pal-KVGSSKR (Pal-SS). Two control peptides were used: an irrelevant sequence from a membrane-adjacent region of another platelet protein, Pal-EIIEDIKRHK (Pal-EII), or KVGFFKR peptide conjugated to a palmityl-like hexadecylamine group moiety on its C-terminus (FF-Pal). Using the protocol illustrated (Figure 1, panel a), we compared the platelet aggregation after 3 min of treatment with buffer (Figure 1, panel b), control peptides (Figure 1, panel c), or Pal-XX peptides alone, with responses obtained following a sequential stimulation with TRAP (10 μM). We demonstrate that the submaximal platelet aggregation obtained by Pal-FF can be enhanced to a full response by the subsequent addition of agonist (Figure 1, panel d). In order to compare the potency of this response across all of our peptides, we recorded the maximal aggregation response to increasing doses of peptide alone after 3 min and plotted results in classical dose–response curves (Figure 1, panels e and f).

The specificity of the aggregation induced by these peptides is demonstrated by the use of the control peptide, KVGFFKR-Pal. This peptide is inactive, demonstrating the importance of the specific orientation of the peptide sequence in producing this pro-thrombotic response. Our previous studies demonstrate that palmityl-peptides remain attached to the platelet phospholipid membrane by virtue of their lipid tail (*18*). Moreover, a maximal response to TRAP is obtained in the presence of this peptide, confirming that the presence of palmitylated peptides does not *per se* affect platelet responses.

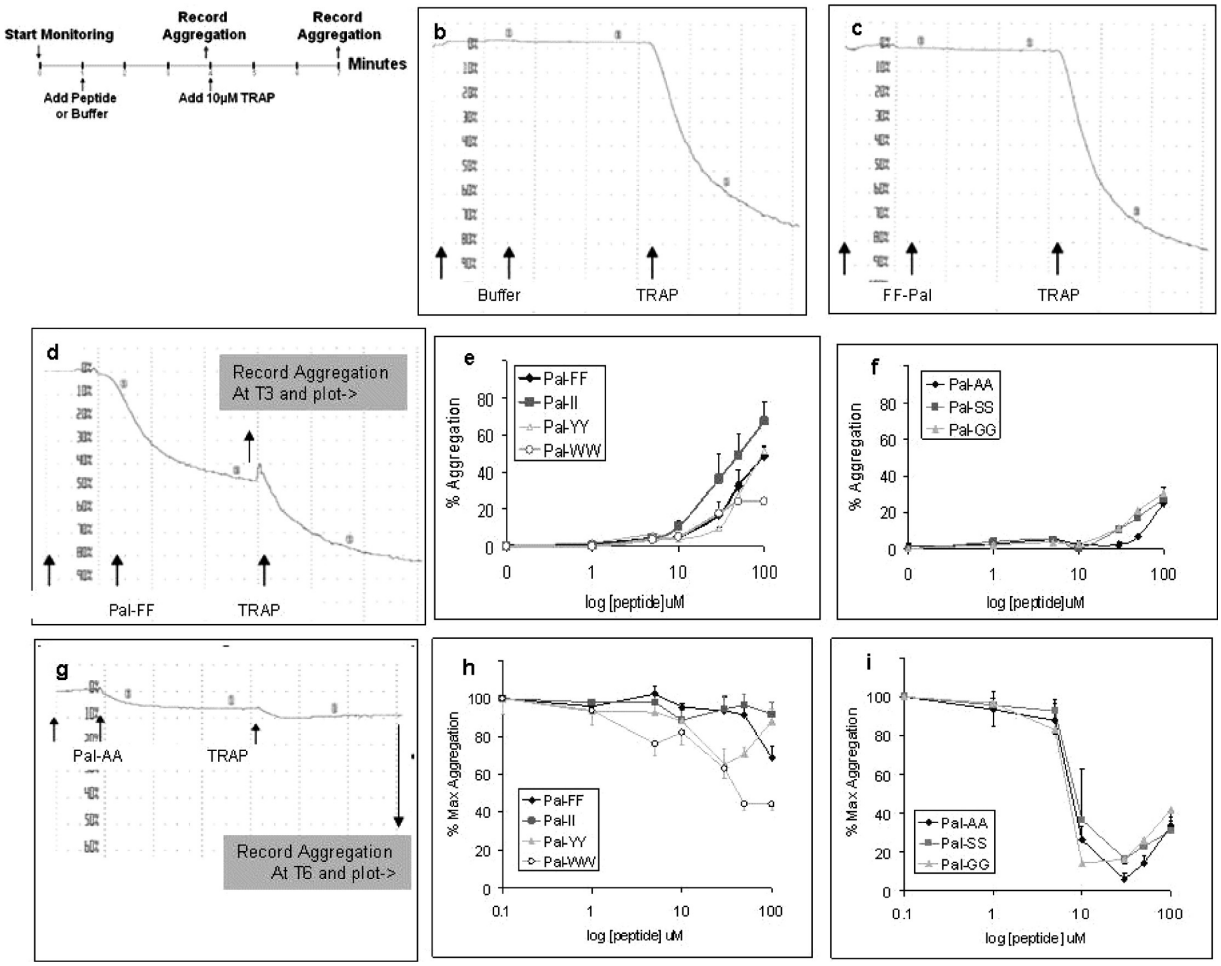

Figure 1. Replacement of the phenylalanine amino acids within the Pal-KVGFFKR sequence reveals an inhibitory potency in these peptides. Washed human platelets (3×10^8 mL^{-1}) were monitored in a Biodata PAP-4 platelet aggregometer according to the timeline in panel a. Real-time recording of platelet aggregation in the presence of (b) buffer or (c) control peptide C-terminally palmitylated KVGFFKR-Pal in the presence or absence of TRAP (10 μM). d) Representative real-time recording of platelet aggregation to Pal-FF (30 μM). e,f) Effects of increasing doses of the indicated peptides on platelet aggregation recorded after 3 min incubation and *before* the addition of TRAP. g) Representative real-time recording of platelet aggregation to Pal-AA (10 μM). h,i) Effects of increasing doses of the indicated peptide on aggregation responses recorded 3 min *after* the addition of TRAP, expressed as a percentage of maximal aggregation. In all cases except Pal-WW, data represent the mean ± SEM of four independent experiments. For the Pal-WW peptide, data represents the mean of duplicate observations of a single dose—response experiment.

Peptides containing hydrophobic or large amino acids (isoleucine, tyrosine, or tryptophan) in place of the phenylalanines are equivalent to the parent Pal-FF peptide in their direct effects on platelet aggregation when added alone and permit a maximal platelet aggregation response when used in combination with TRAP. In contrast, peptides containing small or hydrophilic amino acids (alanine, glycine, or serine) in these positions have weak agonist potency when used alone, especially at concentrations below 50 μM, but surprisingly are potent inhibitors of aggregation responses when used in combination with thrombin or TRAP (Figure 1, panel g). This unexpected result, indicating an inhibitory activity in synthetic integrin-derived peptides, is dose-dependent and reaches a maximal effect, wherein platelet aggregation to TRAP is completely abrogated, at 10 μM peptide (Figure 1, panel i). Some inhibitory activity is observed with the Pal-FF peptide, but only at doses

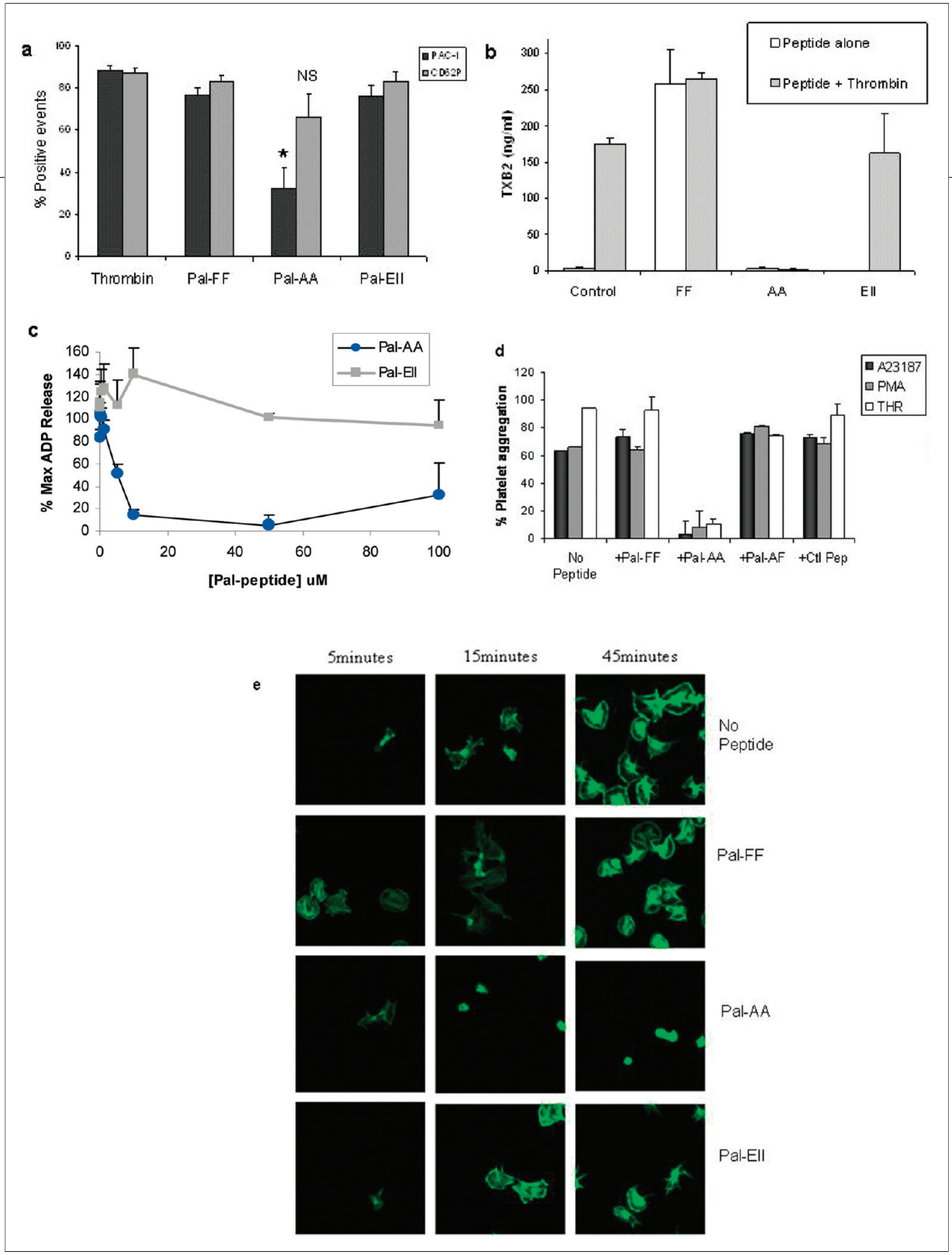

Figure 2. Inhibitory effect of Pal-AA peptide is observed in multiple assays of platelet function. a) Washed platelets were coincubated with peptide (50 μM) and thrombin (0.2 U mL^{-1}) and assayed for integrin activation (PAC-1 antibody) or α-granule secretion (CD62P antibody). b) TXA_2 synthesis was determined in the presence or absence of 0.2 U mL^{-1} thrombin. c) Platelet secretion of ADP was recorded using a chronolume assay in the presence of increasing concentrations of Pal-AA peptide or control (Pal-EII) peptide. d) Platelet aggregation in response to A23187 (0.1 μM, black bar), phorbol 12-myristate 13-acetate (1 μM, gray bar), or thrombin (0.2 U mL^{-1}, white bar) was equally inhibited by Pal-AA peptide (10 μM). Data represent the mean ± SEM for four independent experiments (NS = nonsignificant; * indicates $P < 0.01$; Student's *t* tests). e) Inhibition of platelet spreading by Pal-AA peptides is shown as representative data following incubation for 5, 15, and 45 min on glass slides coated with 20 μg mL^{-1} fibrinogen in the presence of the indicated peptides. Platelets were stained with FITC phalloidin. Panels represent a 50 μm^2 section of the glass slide. Each treatment was performed a minimum of four times.

above 50 μM (Figure 1, panel h). Pal-WW peptide is intermediate in its activity and can cause only a partial inhibition of TRAP-induced platelet aggregation. Thus, all peptides exhibit some degree of agonist action on platelet aggregation, especially at high doses. In contrast, some peptides have an additional inhibitory effect at lower doses.

Pal-AA Inhibits Multiple Platelet Responses to Agonists. Agonist-induced activation of platelets induces TXA_2 synthesis, CD62P surface expression, ADP release, and enhanced binding of the integrin-specific activation-dependent PAC-1 monoclonal antibody (*10, 18, 22, 23*). Here we demonstrate that Pal-AA inhibits all these responses with the single exception of CD62P expression (Figure 2). It is noteworthy that this response is an integrin-independent event in human platelets as α-granule release is unaffected in Glanzmann's patients (*24*). Thus, the opposing agonist and inhibitory effects of the modified integrin-derived peptides are maintained in a number of separate assays of platelet activation (Figure 2, panels a−c). The inhibitory activity of the Pal-AA peptide is also confirmed for other platelet agonists including phorbol 12-myristate 13-acetate (PMA), calcium ionophore (A23187), and thrombin (Figure 2, panel d). In addition, Pal-AA peptide inhibits platelet spreading on an immobilized fibrinogen substrate (Figure 2, panel e). These data imply that the site of the inhibitory action of the peptide is downstream of the well-characterized agonist-stimulated pathways in platelets and occurs subsequent to calcium release and PKC activation.

Pal-AA Peptide Is Not a True Antagonist. To establish if the Pal-AA peptide is a true antagonist of platelet activation, its capacity to inhibit or provoke a phosphotyrosine response in the presence or absence of TRAP (10 μM) was examined. Western blot analysis of platelets lysates prepared after incubation with peptide alone for 3 min and stained with the phosphotyrosine-specific antibody 4G10 is shown in Figure 3, panel a. The profile of the phosphotyrosine response to Pal-FF is similar to that obtained with TRAP alone. However, in contrast, the phosphotyrosine pattern induced by Pal-AA is clearly different, demonstrating reduced phosphorylation of a phosphoprotein at approximately 80 kDa and absence of 100 kDa phosphoprotein. Similar differences in phosphotyrosine profiles are observed when platelets are cotreated with peptides and agonist (Figure 3, panel b). Thus, Pal-AA provokes an altered phosphotyrosine profile in platelets when incubated in the absence of platelet agonists. It is therefore not a true antagonist of integrin activation since, classically, antagonists have no intrinsic activity but merely block an agonist-induced response. Pal-AA must be working *via* preferential interaction with downstream signaling pathways and may promote a physiological counter activity that inhibits platelet function.

Further probing of the phosphotyrosine response to peptide stimulation can enhance our knowledge of the precise pathways involved in this response. FAK phosphorylation is a downstream event in integrin signaling (*25*) that occurs after integrin activation, talin binding, and clustering. Immunoprecipitation of FAK (MW 125 kDa), followed by anti-phosphotyrosine Western blot analysis, showed that Pal-AA failed to support phosphorylation of FAK. Furthermore, TRAP-induced FAK tyrosine phosphorylation was prevented by Pal-AA (Figure 3, panel c). Thus Pal-AA peptide actively diverts the integrin signaling pathways away from focal adhesion pathways. This is entirely consistent with our previous reports that CHO cell lines expressing $\alpha_{IIb}(F^{992}A,F^{993}A)\beta_3$ have impaired cytoskeletal assembly when adhering to immobilized fibrinogen. These data argue strongly against a passive role for the inhibitory peptides, instead suggesting an active involvement in an inhibitory or anti-thrombotic pathway that directly impacts on integrin phosphorylation and downstream events.

Because of the known close association of FAK and α-actinin in the platelet phosphotyrosine cascade (*26*), we also examined phosphorylation of α-actinin (Figure 3, panel d). Phosphorylation of α-actinin (MW 100 kDa) and Syk kinase (MW 72 kDa) were equivalent in the presence of Pal-FF and Pal-AA peptides, suggesting that neither of these proteins are responsible for the altered phosphotyrosine profile observed in Pal-AA-treated platelets. Elucidating the precise molecular pathways by which Pal-FF and Pal-AA peptides mediate their independent effects on platelet function will necessitate further studies.

The inhibitory activity identified for Pal-AA, Pal-SS, and Pal-GG cannot be attributed to a classical antagonist potency of these peptides for two reasons. First, these peptides demonstrate some agonist-like activity at doses of 50 μM and above. Second, classical antagonists should bind to a "receptor" and prevent an agonist-induced response but should have no intrinsic activity by themselves. Pal-AA/GG/SS peptides demon-

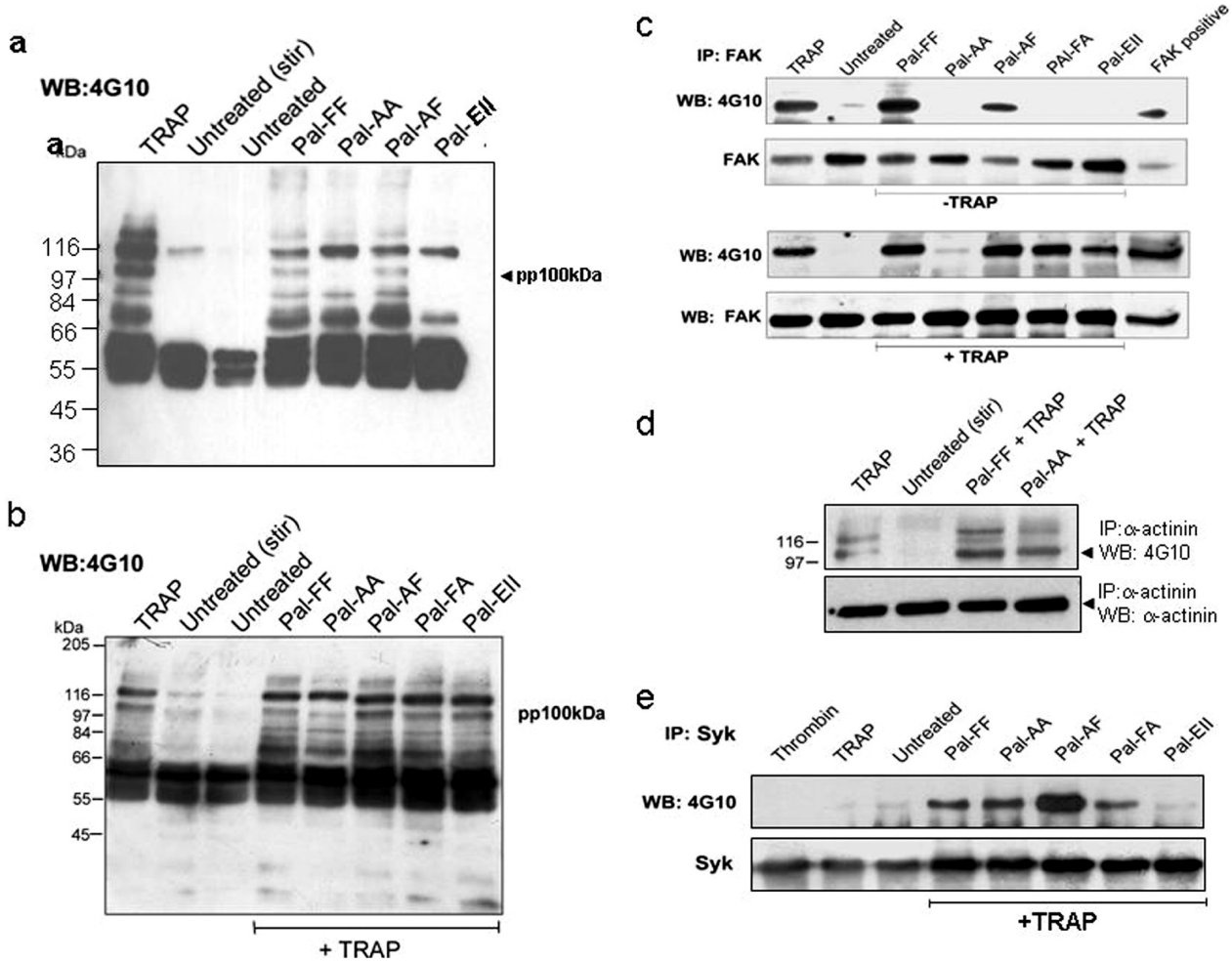

Figure 3. Outside-in tyrosine phosphorylation is differentially modulated by peptide treatment of platelets. Washed platelets (6×10^8 mL^{-1}) were either (a) stimulated with peptide (50 μM) and allowed to aggregate for 3 min or (b) preincubated for 3 min with peptide prior to the addition of TRAP (1 μM) and allowed to aggregate for a further 3 min. Platelet lysates were separated on 7.5% SDS—PAGE gels and Western blotted with a 4G10 anti-phosphotyrosine monoclonal antibody. The Pal-AA peptide caused a reduced phosphotyrosine profile relative to agonist peptides or thrombin, most notably, a protein in the 100 kDa region (arrow). Lysates from washed platelets prepared as in panels a or b were immunoprecipitated with (c) anti-FAK, (d) anti-α-actinin, or (e) anti-Syk antibodies and Western blotted using 4G10 phosphotyrosine specific antibodies (upper panels). Identical samples were probed with antibodies specific to FAK, α-actinin, or Syk to illustrate equal loading (lower panels). Data represents observations from at least three independent experiments.

strate strong intrinsic activity in assays of tyrosine phosphorylation. Thus, these peptides could be described as partial agonists, which are capable of inducing a lesser maximal response than a full agonist but are nonetheless able to induce some responses in the platelet. However, unlike classical partial agonists, Pal-AA/GG/SS can reduce the response to a standard dose of TRAP (10 μM) to less than their own maximal response at low peptide doses. This may be because the system is more complicated than normal, as TRAP is not a direct activator of integrin occupancy but an indirect activator *via* "outside-in" signaling pathways. An alternative explanation is that these peptides (Pal-AA/GG/SS) activate a complementary negative regulatory pathway within platelets and therefore mimic a physiological inhibition of platelet function. Differentiation between these two modes of inhibition must await a more detailed understanding of the precise molecular mecha-

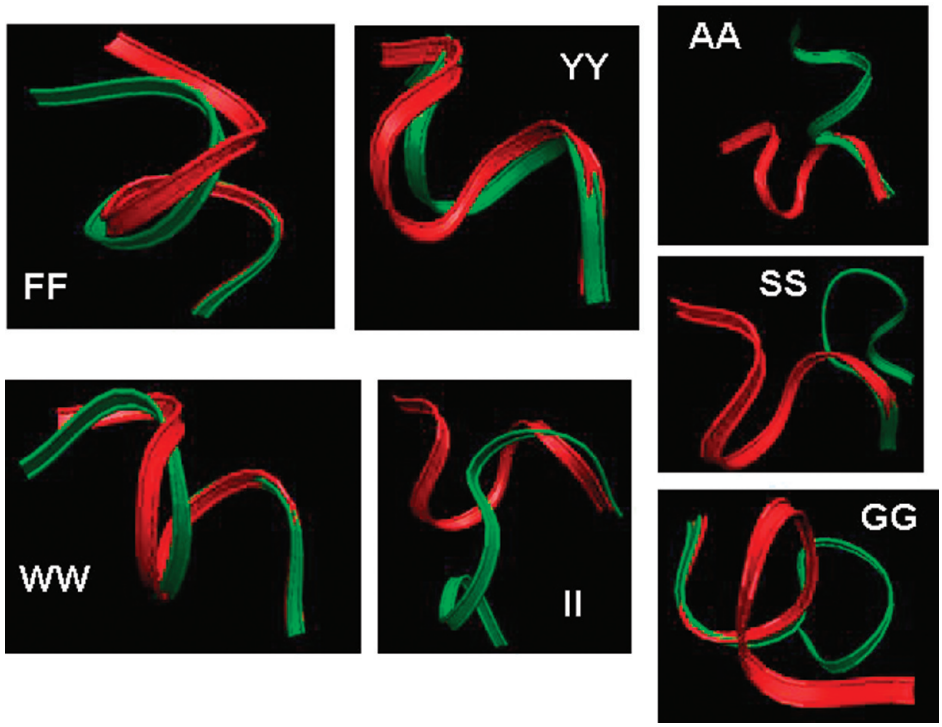

Figure 4. Superposition of KVGXXKR backbones (green) to the 1KUP_KVGFFKR backbone (red). Peptide structures were modeled using the ESYPRED3D program (*35*) and superimposed on the template backbone of the integrin αIIb cytoplasmic (1KUP) (*20*) using the superposition algorithm of VMD (*39*). Details regarding the fit of these models are shown in Table 1.

nisms underlying their actions. Studies are underway in our laboratories to address this issue (*27*).

Structure–activity Relationship of KVGXXKR Peptides. In order to further our understanding of the structure–activity relationship of the integrin cytoplasmic tail peptides, we examined the relationships between the 3D structural parameters of these peptides obtained from their homology models (Figure 4) and their physicochemical parameters derived from various predictions (Table 1) with their biological activity. We postulated that the hydrophobicity might be an important estimator of the biological activity of these synthetic peptides, as it is established that many known interactions with the integrin cytoplasmic tail are hydrophobic in nature (*27, 28*). Because all peptides have dual activity, it was difficult to correlate effects with classical pharmacological parameters such as EC_{50} or IC_{50}. We therefore compared parameters to the observed effects of 30 μM peptide, a dose that clearly delineated an agonist peptide from an inhibitory one. The results obtained indicate that the peptides stratify into agonist or inhibitory peptides depending on the hydrophobicity of the substituted XX residues ($p = 0.009$ and $\rho = 0.74$) and their degree of disorder ($p = 0.015$ and $\rho = 0.71$). No correlation was found between the biological responses of the peptide and other biophysical indices of peptide structure such as aliphatic index, α-helical content or the root-mean-square deviation (rmsd) of the average distance between the backbones of superimposed peptides.

Positive correlations were observed between average backbone extension of peptides with the helical content of the peptide (Agadir index) and their aliphatic indices ($p = 0.0320$ and $\rho = 0.7136$; $p = 0.0069$ and $\rho = 0.7581$, respectively) suggesting that more helical peptides have extended backbones. The superposition of the KVGxxKR backbones to the KVGFFKR portion of the 1KUP template (Figure 4) shows that in most of the cases the peptide backbones fit to the α-helical backbone of the α_{IIb} template. In particular, the native KVG-

TABLE 1. Physicochemical characteristics and 3D structural parameters from homology models for KVGXXKR peptides[a]

	Biological response		Physicochemical properties						Hydrophobicity determination scales					IKUP		
XX	% Agonist response to 30 μM peptide	% Inhibition of TRAP by 30 μM peptide	MW	Theo PI	Instability index	Aliphatic index	GRAVY	Disorder	Eisenberg	Rose	Janin	Engelman	Octanol scale	*E* (kJ/mol)	rmsd (All)	ABE
II	36.32	0.7	813	11.17	6.63	152.86	0.071	0.216	−1.21	5.02	−2.7	−20.1	5.86	148.24	5.03	20.19
FF	16.78	4.2	881	11.17	9.41	41.43	−0.414	0.105	−1.59	5.02	−3.1	−18.9	4.68	77.68	1.88	14.59
WW	17.72	27.3	959.1	11.17	48.51	41.43	−1.471	0.233	−2.35	4.96	−3.5	−22.5	3.92	48.79	2.86	15.77
YY	9.69	34.2	913	10	36.39	41.43	−1.586	0.288	−3.45	4.78	−4.9	−27.7	6.68	−6.19	1.5	15.81
AF	67.18	−6.3	804.9	11.17	−2.71	55.71	−0.557	0.441	−2.16	4.88	−3.3	−21	6.89	132.14	3.88	17.15
FA	21.28	69.7	804.9	11.17	30.89	55.71	−0.557	0.349	−2.16	4.88	−3.3	−21	6.89	58.15	3.07	15.93
SS	10.65	83.2	760.8	11.17	58.4	41.43	−1.443	0.952	−4.33	4.58	−4.3	−25.1	9.02	73.74	5.54	17.77
GG	11.34	83.2	700.8	11.17	54.01	41.43	−1.329	0.868	−3.01	4.7	−3.5	−24.3	10.4	266.47	3.35	15.88
AA	2.49	95.8	728.8	11.17	18.76	70	−0.7	0.780	−2.73	4.74	−3.5	−23.1	9.1	96.95	4.31	17.92
P value			0.308	0.319	0.091	0.731	0.301	**0.015**	**0.037**	**0.006**	**0.060**	**0.035**	**0.009**	0.811	0.699	0.184
ρ			−0.339	−0.332	0.534	0.118	−0.343	0.706	−0.632	−0.771	−0.582	−0.636	0.741	−0.082	0.132	0.433

[a]MW refers to peptide molecular weight; Theo PI is the theoretical isoelectric point of each peptide; GRAVY is the grand average of hydropathy index. These parameters are determined as described in Methods. Eisenberg, Rose, Janin, Engleman, and Octanol are different hydrophobicity indices. ABE is the average backbone extension for peptides built on the 1KUP template. *P* values and Spearman ρ values are statistical correlations of the indicated parameter with the capacity of each peptide to inhibit TRAP-induced platelet aggregation. Additional information and fits to other pdb models are available in the Supplementary Table. Bold text indicates statistically significant P value compared to the biological response.

FFKR peptide sequence yields a structure corresponding to the published IKUP structure. However, peptide models lacking hydrophobic amino acids showed much greater structural divergence from the 1KUP template KVGFFKR region of the α_{IIb} cytoplasmic tail. This lack of conformity correlates with the observed difference in biological activity of these peptides. Thus the structural analysis of the peptides suggests that hydrophobicity and peptide disorder are the most important predictors of potency. However, relative hydrophobicity within this group did not predict the rank order of potency, suggesting that additional factors also contribute to the response.

Although tryptophan is considered to be a hydrophobic amino acid, the biological activity of Pal-KVGWWKR peptide is observed to be less than would be expected. It is interesting to note therefore that the two aromatic tryptophan residues stack on top of each other (Figure 4), resulting in a more contracted backbone. This is also evident from the distance between the aromatic centroids (2.9417 Å for the tryptophan centroids in the KVGWWKR peptide). Such a stacking interaction is absent in the Pal-KVGYYKR and Pal-KVGFFKR peptides, as evident from their respective centroid−centroid distances (7.2915 and 8.0498 Å, respectively), and may explain the differences in activity.

Cell Permeability of Pal-KVGXXKR Peptides. All peptides tested, both activatory and inhibitory, showed a very high capacity to associate with cell membranes, suggesting similar capacity to permeate a biological cell membrane. Red blood cells (RBCs) were used as model cell membranes in these experiments. The cell permeability of the palmitylated peptides, but not the nonpalmitylated control peptides, is evident from the HPLC and ^{1}H NMR spectral images (Figure 5). The disappearance of the peptide peaks in the HPLC chromatograms and the absence of specific palmityl resonances in the ^{1}H NMR spectra after the addition of RBCs demonstrate that the palmitylated peptides are no longer present in abundance in solution but have associated with the RBC membrane or translocated into the cell. In contrast, in the control peptides (without palmityl tag), the peptide peaks are clearly visible in solution even 15 min after the addition of RBCs. Because palmityl-peptides can

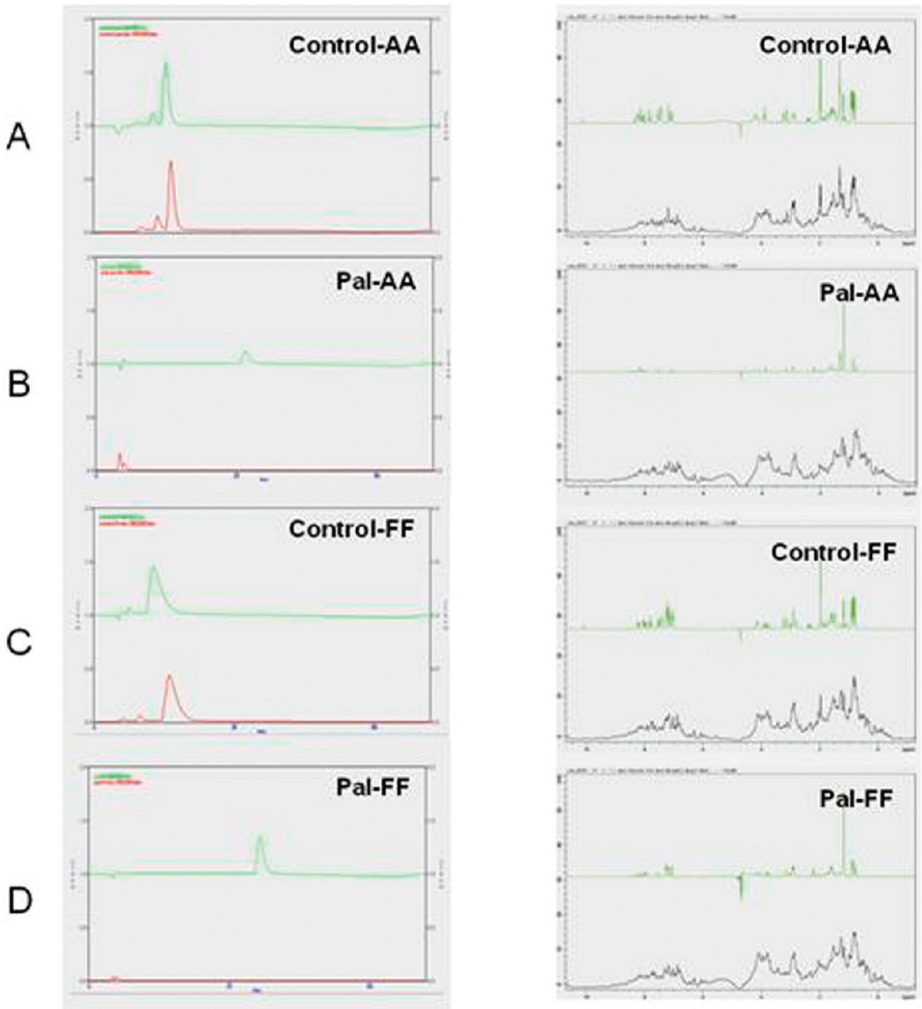

Figure 5. Palmitylated peptides but not non-palmitylated peptides are membrane-permeable. Pal-KVGFFKR peptide (Pal-FF, 1 mM), Pal-KVGAAKR (Pal-AA, 1 mM), or corresponding unpalmitylated control peptide containing an additional 4 amino acids at the N-terminal domain, Ac-LAMWKVGFFKR (Control-FF, 1 mM) or Ac-LAMWKVGAAKR (Control-AA, 1 mM) were incubated with washed RBCs for 15 min at 37 °C. For HPLC analysis (left panels), RBCs were removed by centrifugation and the peptide present in the supernatant was separated on a Jupiter C5 250 mm × 4.6 mm column with a 40 min gradient of water/acetonitrile of 70/30 to 15/85. Data is shown as red lines. For comparison, the chromatogram of peptide alone is shown as green lines. In parallel experiments, peptides were analyzed alone (green lines) or in the presence of RBCs (black lines) by ^{1}H NMR with D_2O as a reference. The absence of specific palmityl resonances in the ^{1}H NMR spectra after the addition of RBCs demonstrates that the palmitylated peptides are no longer present in abundance in solution but have associated with the RBC membrane or translocated into the cell. In contrast, in the control peptides (without palmityl tag), the peptide peaks are clearly visible in solution even 15 min after the addition of RBCs.

cause cell lysis at the high concentrations necessary for detection, additional peaks are present in the spectra after the addition of RBC (right panel B and D, black spectra) that are neither present in the peptides alone nor present in the background spectrum for RBC alone. At the concentrations used in platelet function assays (1−50 μM), no lysis is observed in RBCs. No significant extra protein peaks have been observed for the control peptides after the addition of RBCs (right panel A and C, black spectra), verifying that nonpalmitylated peptides

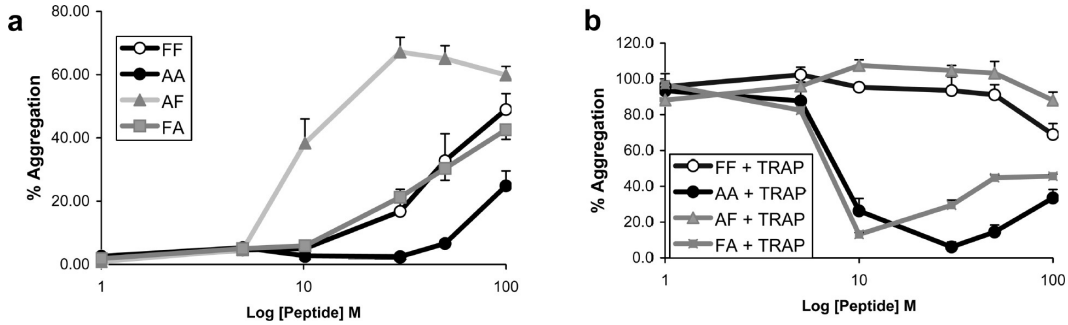

Figure 6. Pal-FA and Pal-AF have opposite biological effects. Platelet aggregation was monitored in washed human platelets (3×10^8 mL^{-1}) according to the timeline in Figure 1, panel a. a) Indicated concentrations of Pal-AF and Pal-FA peptides were incubated for 3 min, and effects recorded before the addition of TRAP. Pal AA and Pal FF are shown for reference. b) Inhibitory effects of the peptides on aggregation responses, recorded 3 min after the addition of TRAP. Data represent the mean ± SEM of 3 or 4 independent experiments.

both remain in solution and have no effect on the integrity of the RBC membrane. In the control peptides, the acetyl resonances at 2 ppm are still present 15 min after the addition of RBCs (right panel A and C, green spectra), thereby proving that these peptides still remain in solution to be detected by NMR. In contrast, the palmityl methylene resonances at 1.2 ppm are not observed in the presence of RBCs, suggesting that the palmitylated peptides have permeated the cell membrane and are no longer available in solution to be detected by NMR. Similar experiments were performed with synthetic liposomes and demonstrated that only palmitylated peptides but not-nonpalmitylated peptides associated with the liposomes (data not shown). There was no difference quantitatively between agonist and inhibitory peptides, typified by Pal-FF and Pal-AA, in their ability to associate with cell membranes. Finally, we have previously demonstrated that fluorescently tagged palmityl-peptides associate with the membrane of platelets or cells, suggesting the lipid tail confines the peptides to the juxta-membranous region in cells (*18*).

Pal-FA and Pal-AF Have Opposite Biological Effects. NMR structural analysis of the α-integrin cytoplasmic tail indicates that the hydrophobic amino acids F^{992} and F^{993} within the α-integrin regulatory motif provide crucial hydrophobic contacts with the β_3 tail that facilitate the maintenance of a resting integrin structural conformation (*19, 20, 29*). In particular, Vinogradova *et al.* demonstrate that F^{992} forms hydrophobic contacts with β_3 (I^{721}) and β_3 (H^{722}). These interactions normally maintain the integrin in a resting conformation. Disruption of these interactions by the introduction of mutations including $F^{992}A$ perturbs the αβ interface and can initiate the "inside-out" signaling that culminates in activation (*8*). According to this model, F^{993} is involved in interactions with distal regions of the α_{IIb} cytoplasmic tail, namely, α_{IIb}-P^{1000} and -D^{1004}. In contrast, Weilje *et al.* identified F^{993} but not F^{992} as central to the dimer interface between integrin αβ cytoplasmic tails (*20*). The crucial difference between the Vinogradova and Weilje studies is the use by the latter of truncated peptide sequences that lack the C-terminal portions of the integrin cytoplasmic tails. However, both studies concurred that additional interactions were also mediated between α_{IIb}-V^{990} and -R^{995} with residues 719−725 of the β_3 subunit. Thus it seems that, when present, the charged C-terminal tails of the α-integrin form strong associations with F^{993}. When absent, the F^{993} residue is free to interact with the β-cytoplasmic tail. These data indicate that within the integrin cytoplasmic tails, the capacity for more than one specific orientation of the peptide tails exists. Cell-permeable peptides containing single substitution of amino acids to yield Pal-FA and Pal-AF peptides also demonstrates preferential roles for the individual amino acids in platelet agonist or inhibitory activity, respectively (Figure 6, panels a and b). These results demonstrate that the biological responses are differentially modulated by each phenylalanine: the first phenylalanine, F^{992}, is critical for inhibitory potency (its absence in Pal-AF yields a peptide with no inhibitory activity, whereas its presence in Pal-FA reveals a potent inhibitory effect), while the second phenylalanine, F^{993}, is critical for an agonist response (its absence in Pal-FA yields a peptide with little agonist potency, whereas its presence in Pal-AF permits a potent agonist response unaffected by the inhibitory effect of F^{992}). Thus, we can

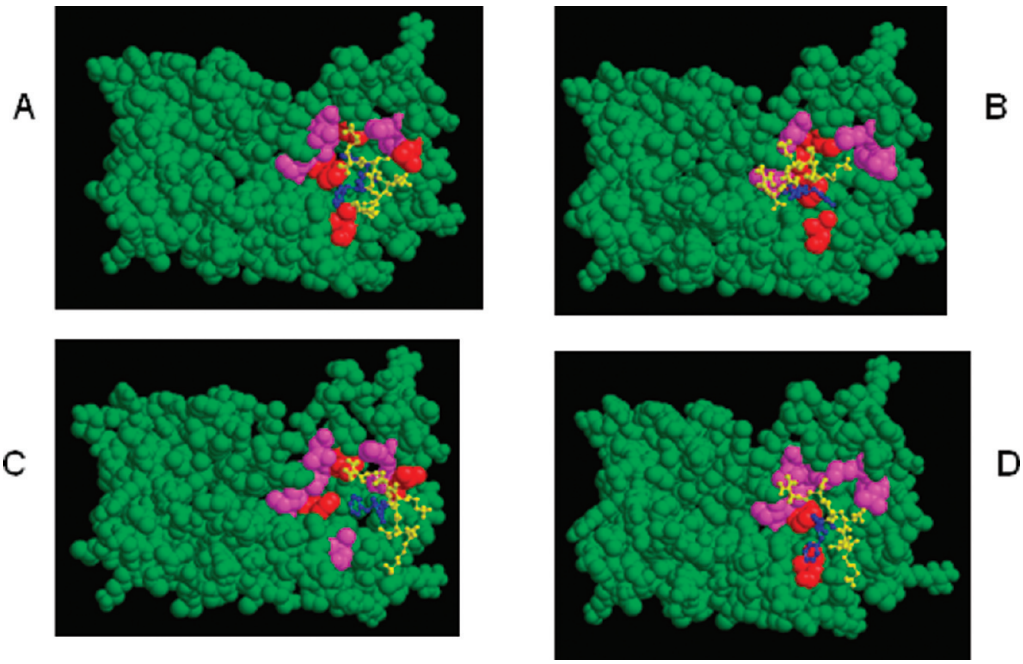

Figure 7. Molecular docking of peptides onto the structure of CIB1. A) CIB1-FF Model-1 (*E* = −9524.085 kJ/mol). B) CIB1-FF Model-2 (*E* = −9464.827 kJ/mol). C) CIB1-FA Model (*E* = −9416.685 kJ/mol). D) CIB1-AF Model (*E* = −9464.156 kJ/mol). Green spheres: CIB1 residues (other than those reported by Barry *et al.* as important). Pink spheres: CIB1 residues (reported by Barry *et al.* but not identified as interacting in our models). Red spheres: CIB1 residues (reported by Barry *et al.* and identified as interacting in our models). Yellow ball and stick: KVGKR residues. Blue ball and stick: XX residues (XX = FF in panels A and B, FA in panel C, and AF in panel D).

conclude that F^{992} presents an inhibitory switch in these peptides. In contrast, F^{993} presents an activation switch. The presence of both phenylalanines probably allows regulatory control of downstream integrin signaling pathways.

The downstream molecular mechanisms underlying the effects of these peptides are not currently known. However, the differential activatory or inhibitory effects of the Pal-KVGxxKR peptides may be due to differential interference with known integrin αβ subunit interactions. Thus, peptides may interfere with the capacity of the α-integrin helical region to interact with the corresponding β-integrin membrane-proximal region by competitively displacing essential contacts with $\alpha_{IIb}V^{990}$ and R^{995}. Pal-AF peptide would be expected to selectively interfere with molecular contacts normally established by $\alpha_{IIb}F^{993}$. Consequently, in the resting integrin conformation, Pal-AF may interfere with the long-range contacts between F^{993}, P^{1000}, and D^{1004} (Vinogradova model), forcing an activated conformation in the integrin cytoplasmic tail and exposing it for binding to any one of a number of known integrin-regulatory proteins such as CIB1 (*11*), PP1c (*13*), ICln (*15*), AUP-1 (*12*), TIM (*17*), or RN181 (*16*). In contrast, Pal-FA may be unable to compete for these F^{993}-specific contacts, explaining the differences in the relative activity of these two peptides. However, in this simple model, it is impossible to explain why or how Pal-AF peptide is more potent than Pal-FF at inducing an agonist response. Similarly, the inhibitory potencies of Pal-FA and Pal-AA peptides are difficult to explain using this simple model.

It is therefore necessary to invoke an alternate model that contains a negative regulatory step (Figure 8, panels C and D). In such a model, Pal-FF peptide mimics the effect of a positive regulatory pathway by interacting with one set of downstream protein interactors. In contrast, Pal-AA interacts with a different set of downstream proteins and provokes an inhibitory response. There is strong recent evidence for a number of diverse integrin -binding proteins in the platelet and other systems. For example, we have demonstrated novel interactions of the KVGFFKR integrin motif with a chloride channel regu-

lator and a ubiquitin pathway modifier (*15, 16*). Here we demonstrate using molecular docking that a KVGFFKR peptide will dock efficiently and with low energy onto the structure of CIB1, the best characterized of all α-integrin-binding proteins. Two different low-energy models of KVGFFKR are presented in Figure 7, panels A and B. This short peptide forms contact with 6 or 7 of the 10 CIB1 residues identified by Barry *et al.* (*28*) as essential for interaction with the entire α_{IIb} tail. In contrast, KVGAFKR and KVGFAKR demonstrate contacts with only three CIB1 residues or four CIB1 residues, respectively, although the predicted energy of interaction is equivocal. As a result, it can be expected that the interaction of these peptides with CIB1 and by inference with other known integrin-binding proteins is altered by subtle changes in the amino acid sequence. Studies are currently underway to elucidate the preferred molecular partners for native and altered integrin tails (*27*). Pal-XX peptides will provide ideal tools for interrogating these pathways.

In summary, we have explored the functionality of an evolutionarily conserved regulatory region of the α-integrin cytoplasmic tail in isolation. By using cell-permeable peptides, we demonstrate that this motif acts as a pivot point for regulation of activatory or inhibitory downstream signaling events in the human platelet. Activity is critically dependent on the central hydrophobic diphenylalanine motif and can be qualitatively tuned by careful selection of replacement amino acids within the sequence. In separate studies, we have shown that this region acts as a binding hub for many different cytosolic proteins in the course of platelet activation (*15, 16, 27*). Together this implies that the Pal-XX peptides will be useful tools for the identification and interrogation of the signaling pathways that promote (Pal-FF, -II, -YY) or inhibit (Pal-AA, -GG, -SS) platelet function. This peptide study has identified a previously unknown functionality in the KVGFFKR motif, in that qualitative disruption of specific interactions involving the hydrophobic phenylalanines reveals novel aspects of integrin signaling pathways that have a negative regulatory role on integrin function and platelet aggregation. Therapeutic agents derived from the inhibitory peptides described in this study may represent a new therapeutic strategy for anti-platelet or anti-integrin drugs.

METHODS

Antibodies and Reagents. All reagents were obtained from Sigma. Antibodies: PAC-1-FITC and CD41a-PE from Becton Dickinson (Oxford, UK); 4G10 anti-phosphotyrosine monoclonal antibody and anti-FAK (clone 4.47) from Upstate Biotechnology (Lake Placid, NY); CD41a from Immunotech (Marseille, France); horseradish peroxidase-conjugated secondary antibody and SuperSignal West Pico from Pierce (Rockford, IL).

Peptide Synthesis and Purification. TRAP (SFLLRN) and integrin-derived KVGXXKR peptides were synthesized as previously described (*10, 23*). Integrin-derived peptides were N-terminally palmitylated and amidated at the C-terminus. Control peptides are either Pal-EII: Pal-EIIEDIKRHK or FF-Pal: KVGFFKR-Pal. Peptides were purified using reversed phase HPLC on Phenomenex Jupiter 5 μm C5 300 Å columns, and their masses were confirmed using a Bruker Reflex III MALDI-TOF mass spectrometer.

Platelet Function Assays. Platelet aggregation was monitored in washed human platelets as previously described (*18*). Briefly, 250 μL of washed platelets (3×10^8 mL^{-1}) were stirred at 1100 rpm at 37 °C for 1 min before the addition of peptide (1−100 μM) for 3 min, followed by addition of TRAP (SFLLRN; 10 μM) for a further 3 min. Thus for each peptide, two dose−response curves were generated recording the response of the platelets to increasing doses of peptide alone and the responses of the platelets to the peptide in the presence of agonist. For thromboxane determination, thromboxane B_2, the stable metabolite of thromboxane A_2, was determined by ELISA (Assay Designs, Inc.; Ann Arbor, MI). Platelet adhesion assays were performed as previously described (*10*). Adherent platelets were stained with FITC phalloidin and analyzed by confocal fluorescent microscopy on a Zeiss LSM500 microscope. FITC-PAC-1 was used as a marker for integrin activation, and PE-labeled CD62P was used as a marker for α-granule secretion. Flow cytometry was used to determine the activation state of both of these markers as described previously (*22*). Data acquisition and analysis were performed with Cell Quest software on a Becton-Dickinson FACS-Calibur flow cytometer at 488/510 nm. ADP release was monitored using a chronolume assay (*23*).

Immunoprecipitation and Immunoblotting. Samples from aggregation assays were solubilized in ice-cold 10X lysis buffer (50 mM ethylmaleimide, 10% Triton-X-100, 5% *N*-octylglucoside, 10 mM sodium orthovanadate, 20 mM PMSF, 200 μg mL^{-1} soya bean trypsin inhibitor, 10 mM EDTA, 100 mM benzamidine, pH 7.4) for 1 h and stored at −80 °C until needed. Platelet lysates were separated on 7.5% SDS acrylamide gels with or without prior immunoprecipitation and transferred onto PVDF. After transfer, the PVDF membrane was blocked with 5% BSA for 2 h and washed with NT buffer (100 mM NaCl, 10 mM Tris-HCl, 0.1% IGPAL). The membrane was incubated with the monoclonal antibody 4G10 (1/2000) for 2 h followed by secondary antibody (goat anti-mouse conjugated with horseradish peroxidase [1/20000]) for 1 h and washed with NT buffer and developed with SuperSignal.

Primary Sequence Analysis, 3D Structural Modeling, and Protein−Protein Docking. The biophysical characteristics of the peptides were calculated using EMBOSS (European Molecular Biology Open Software Suite) (*30, 31*). In addition, hydrophobicity was computed from an optimal hydrophobicity scale based on 28 published scales (*32*). The packing average (average backbone extension, ABE) defined as the mean pairwise

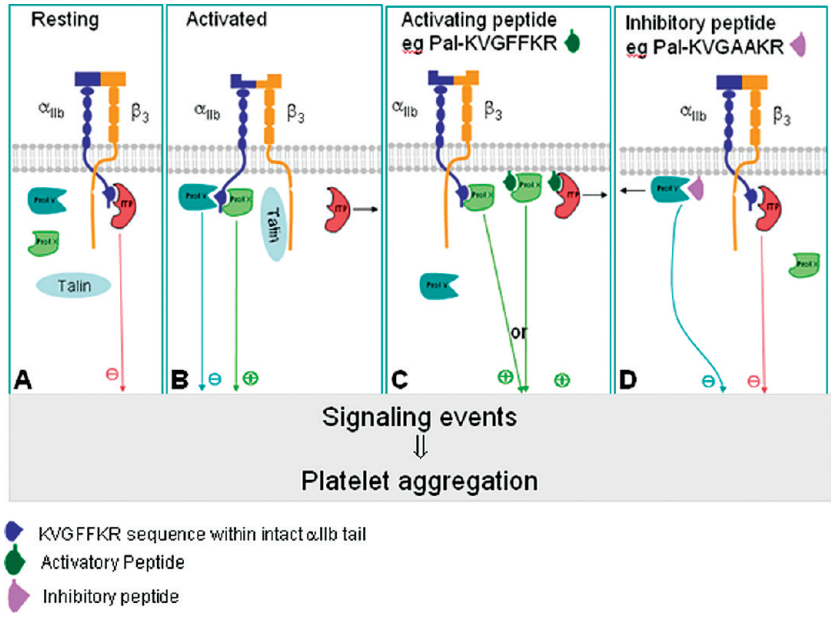

Figure 8. Model showing a possible mechanism of action for activatory and inhibitory peptides. A) In resting platelets, the integrin αIIbβ3 is maintained in a resting conformation through an interaction with an integrin tethering protein (ITP). Association of ITP with the integrin cytoplasmic tails promotes inhibitory signals that prevent platelet activation. Other proteins capable of binding to the integrin are present in the platelet cytoplasm but are precluded from interacting with the integrin cytoplasmic tails. Such proteins are indicated as Protein X, Protein Y, and Talin. Proteins X and Y may represent families of proteins. B) In activated platelets it is established that the integrin cytoplasmic tails undergo a conformational change and bind talin (*19*). We previously proposed that this was due to a dissociation of the ITP, an event that then allows access of other integrin-binding proteins such as talin and Proteins X and Y. In this model we propose that proteins in the X family promote integrin signaling events that result in platelet aggregation and proteins in the Y family inhibit these events. A balance between inhibitory and activatory signals determines the degree of platelet activation. C) Dissociation of ITP is accelerated by the activating peptide pal-KVGFFKR (*18*) allowing access of Protein X to the untethered αIIb cytoplasmic tail and thus promoting an activatory pathway resulting in platelet aggregation. D) In contrast, the inhibitory peptide, pal-KVGAAKR, is unable to dissociate ITP from its binding site but has enhanced affinity for the inhibitory Protein Y family, resulting in an inhibition of platelet aggregation. Alternatively, pal-KVGFFKR and other activating peptides may bind to Protein X > Protein Y, promoting platelet activation (panel C), whereas inhibitory peptides may have a greater affinity for the Protein Y family than for the Protein X family, thus resulting in an inhibition of platelet activation (panel D).

distance between all C_α atoms of each heptamer peptide, calculated as $(\sum[(x_1 - x_2)^2 + (y_1 - y_2)^2 + (z_1 - z_2)^2]^{1/2})/21$ was calculated for all these 3D models. The 3D structures of the peptide homology models were superimposed to the KVGFFKR backbone in each of the four templates using the SUPERPOSE algorithm (*33*) to obtain their rmsd values. Short signaling motifs often occur in disordered regions of peptides; hence we have calculated the IUPRED disorder prediction for each of the KVGXXKR sequences studied (*34*). The statistical analyses was carried out using STATA 8.0 (Stata Corporation, TX). Homology models of KVGXXKR (XX = FF, FA, and AF) peptides were generated using the 1KUP KVGFFR backbone using ESYPRED3D algorithm (*35*). These models were then docked to CIB using Cluspro algorithm (*36, 37*). The 3D images of CIB-KVGXXKR (XX = FF, FA, AF) were generated using RASMOL (*38*).

HPLC Analysis of Peptide Permeability. One agonist peptide (Pal-FF; 1 mM), one antagonist peptide (Pal-AA; 1 mM), and their non-palmitylated controls (1 mM each) were analyzed alone using high performance liquid chromatography (HPLC) on a PerSeptive Biosystems BioCad/Sprint chromatography system using a Jupiter C5 250 × 4.6 mm column with a 40 min gradient of water/acetonitrile 70/30 to 15/85, to obtain a chromatogram of each peptide. Red blood cells (RBC), obtained from blood withdrawn in sodium citrate anticoagulant, were washed 4 times with PBS and adjusted to 1.2×10^6 μL^{-1}. Peptides, at a final concentration of 1 mM, were added to 300 μL of RBCs and incubated at 37 °C for 15 min. RBCs are precipitated by centrifugation at 150*g* for 5 min. The supernatant was filtered on an Amicon Ultra centrifugal filter unit with a molecular weight cut-off of 10 kDa to remove any contaminants. The clear filtrate obtained was injected on HPLC using the same conditions as for peptides alone.

NMR Analysis of Peptide Permeability. The ^1H NMR spectra of Pal-FF, Pal-AA and the two control peptides, Ac-LAMWKVGFFKR

and Ac-LAMWKVGAAKR (1 mM), were recorded using Bruker Avance II 600 NMR triple resonance cryoprobe NMR spectrometer. The RBCs used were prepared as described for the HPLC experiments. A first spectrum of a background of RBC was recorded as following: 450 μL of RBC + 50 μL of D_2O were added to a NMR tube, and the ^1H NMR spectrum was recorded. Peptide-alone ^1H NMR spectra were also recorded for each peptide at a concentration of 1.2 mM as reference. After this recording, 50 μL of RBC was added to the same tube, and NMR spectra were recorded for the peptides in the presence of RBC immediately after addition and every 3 min up to 15 min.

Acknowledgment: The authors acknowledge the assistance of Dr. Achim Treumann for MS analysis of peptides and Dr. John O'Brien, Senior Experimental officer, NMR facility, Trinity College Dublin for his assistance in recording the ^1H NMR spectra. The research is supported by grants from The Health Research Board Ireland (N.M., M.R., C.T.O'D., K.A., and E.B.), Science Foundation Ireland (N.M., T.K., L.C., D.S.), the Higher Education Authority of Ireland (M.D. and N.M.), and postdoctoral fellowships under the EU Marie Curie RTN scheme (H.D., E.B., and M.R.).

Supporting Information Available: This material is available free of charge *via* the Internet at http://pubs.acs.org.

REFERENCES

1. Newby, L. K., Califf, R. M., White, H. D., Harrington, R. A., Van de Werf, F., Granger, C. B., Simes, R. J., Hasselblad, V., and Armstrong, P. W. (2002) The failure of orally administered glycoprotein IIb/IIIa inhibitors to prevent recurrent cardiac events, *Am. J. Med. 112*, (8), 647–658.
2. Bassler, N., Loeffler, C., Mangin, P., Yuan, Y., Schwarz, M., Hagemeyer, C. E., Eisenhardt, S. U., Ahrens, I., Bode, C., Jackson, S. P., and Peter, K. (2007) A mechanistic model for paradoxical platelet activation by ligand-mimetic alphaIIb beta3 (GPIIb/IIIa) antagonists, *Arterioscler., Thromb., Vasc. Biol. 27*, (3), e9–e15.
3. O'Toole, T. E., Katagiri, Y., Faull, R. J., Peter, K., Tamura, R., Quaranta, V., Loftus, J. C., Shattil, S. J., and Ginsberg, M. H. (1994) Integrin cytoplasmic domains mediate inside-out signal transduction, *J. Cell Biol. 124*, (6), 1047–1059.
4. Peter, K., and Bode, C. (1996) A deletion in the alpha subunit locks platelet integrin alpha IIb beta 3 into a high affinity state, *Blood Coagulation Fibrinolysis 7*, (2), 233–236.
5. Hughes, P. E., and Pfaff, M. (1998) Integrin affinity modulation, *Trends Cell Biol. 8*, (9), 359–364.
6. Lu, C., Takagi, J., and Springer, T. A. (2001) Association of the membrane proximal regions of the alpha and beta subunit cytoplasmic domains constrains an integrin in the inactive state, *J. Biol. Chem. 276*, (18), 14642–14648.
7. Kim, M., Carman, C. V., and Springer, T. A. (2003) Bidirectional transmembrane signaling by cytoplasmic domain separation in integrins, *Science 301*, (5640), 1720–1725.
8. Ma, Y. Q., Yang, J., Pesho, M. M., Vinogradova, O., Qin, J., and Plow, E. F. (2006) Regulation of integrin alphaIIbbeta3 activation by distinct regions of its cytoplasmic tails, *Biochemistry 45*, (21), 6656–6662.
9. Ginsberg, M. H., Partridge, A., and Shattil, S. J. (2005) Integrin regulation, *Curr. Opin. Cell Biol. 17*, (5), 509–516.
10. Aylward, K., Meade, G., Ahrens, I., Devocelle, M., and Moran, N. (2006) A novel functional role for the highly conserved alpha-subunit KVGFFKR motif distinct from integrin alphaIIbbeta3 activation processes, *J. Thromb. Haemostasis 4*, (8), 1804–1812.
11. Naik, U. P., Patel, P. M., and Parise, L. V. (1997) Identification of a novel calcium-binding protein that interacts with the integrin alphaIIb cytoplasmic domain, *J. Biol. Chem. 272*, (8), 4651–4654.
12. Kato, A., Kawamata, N., Tamayose, K., Egashira, M., Miura, R., Fujimura, T., Murayama, K., and Oshimi, K. (2002) Ancient ubiquitous protein 1 binds to the conserved membrane-proximal sequence of the cytoplasmic tail of the integrin alpha subunits that plays a crucial role in the inside-out signaling of alpha IIbbeta 3, *J. Biol. Chem. 277*, (32), 28934–28941.
13. Vijayan, K. V., Liu, Y., Li, T. T., and Bray, P. F. (2004) Protein phosphatase 1 associates with the integrin alphaIIb subunit and regulates signaling, *J. Biol. Chem. 279*, (32), 33039–33042.
14. Gushiken, F. C., Patel, V., Liu, Y., Pradhan, S., Bergeron, A. L., Peng, Y., and Vijayan, K. V. (2008) Protein phosphatase 2A negatively regulates integrin alpha IIb beta 3 signaling, *J. Biol. Chem. 283*, (19), 12862–12869.
15. Larkin, D., Murphy, D., Reilly, D. F., Cahill, M., Sattler, E., Harriott, P., Cahill, D. J., and Moran, N. (2004) ICln, a novel integrin alphaIIbbeta3-associated protein, functionally regulates platelet activation, *J. Biol. Chem. 279*, (26), 27286–27293.
16. Brophy, T. M., Raab, M., Daxecker, H., Culligan, K. G., Lehmann, I., Chubb, A. J., Treumann, A., and Moran, N. (2008) RN181, a novel ubiquitin E3 ligase that interacts with the KVGFFKR motif of platelet integrin alpha(IIb)beta3, *Biochem. Biophys. Res. Commun. 369*, (4), 1088–1093.
17. Liu, Q. Y., Corjay, M., Feuerstein, G. Z., and Nambi, P. (2006) Identification and characterization of triosephosphate isomerase that specifically interacts with the integrin alphaIIb cytoplasmic domain, *Biochem. Pharmacol. 72*, (5), 551–557.
18. Stephens, G., O'Luanaigh, N., Reilly, D., Harriott, P., Walker, B., Fitzgerald, D., and Moran, N. (1998) A sequence within the cytoplasmic tail of GpIIb independently activates platelet aggregation and thromboxane synthesis, *J. Biol. Chem. 273*, (32), 20317–20322.
19. Vinogradova, O., Velyvis, A., Velyviene, A., Hu, B., Haas, T., Plow, E., and Qin, J. (2002) A structural mechanism of integrin alpha(IIb) beta(3) "inside-out" activation as regulated by its cytoplasmic face, *Cell 110*, (5), 587–597.
20. Weljie, A. M., Hwang, P. M., and Vogel, H. J. (2002) Solution structures of the cytoplasmic tail complex from platelet integrin alpha IIb- and beta 3-subunits, *Proc. Natl. Acad. Sci. U.S.A. 99*, (9), 5878–5883.
21. De Melker, A. A., Kramer, D., Kuikman, I., and Sonnenberg, A. (1997) The two phenylalanines in the GFFKR motif of the integrin alpha6A subunit are essential for heterodimerization, *Biochem. J. 328*, (Pt 2), 529–537.
22. Walsh, G. M., Sheehan, D., Kinsella, A., Moran, N., and O'Neill, S. (2004) Redox modulation of integrin $\alpha_{IIb}\beta_3$ involves a novel allosteric regulation of its thiol isomerase activity, *Biochemistry 43*, (2), 473–480.
23. Edwards, R. J., Moran, N., Devocelle, M., Kiernan, A., Meade, G., Signac, W., Foy, M., Park, S. D., Dunne, E., Kenny, D., and Shields, D. C. (2007) Bioinformatic discovery of novel bioactive peptides, *Nat. Chem. Biol. 3*, (2), 108–112.
24. Fullard, J. F. (2004) The role of the platelet glycoprotein IIb/IIIa in thrombosis and haemostasis, *Curr. Pharm. Des. 10*, (14), 1567–1576.
25. Zhang, X., Jiang, G., Cai, Y., Monkley, S. J., Critchley, D. R., and Sheetz, M. P. (2008) Talin depletion reveals independence of initial cell spreading from integrin activation and traction, *Nat. Cell Biol. 10*, 1062–1068.
26. Izaguirre, G., Aguirre, L., Hu, Y. P., Lee, H. Y., Schlaepfer, D. D., Aneskievich, B. J., and Haimovich, B. (2001) The cytoskeletal/non-muscle isoform of alpha-actinin is phosphorylated on its actin-binding domain by the focal adhesion kinase, *J. Biol. Chem. 276*, (31), 28676–28685.

27. Daxecker, H., Raab, M., Bernard, E., Devocelle, M., Treumann, A., and Moran, N. (2008) A peptide affinity column for the identification of integrin alpha IIb-binding proteins, *Anal. Biochem. 374*, (1), 203–212.
28. Barry, W. T., Boudignon-Proudhon, C., Shock, D. D., McFadden, A., Weiss, J. M., Sondek, J., and Parise, L. V. (2002) Molecular basis of CIB binding to the integrin alpha IIb cytoplasmic domain, *J. Biol. Chem. 277*, (32), 28877–28883.
29. Vinogradova, O., Haas, T., Plow, E. F., and Qin, J. (2000) A structural basis for integrin activation by the cytoplasmic tail of the alpha IIb-subunit, *Proc. Natl. Acad. Sci. U.S.A. 97*, (4), 1450–1455.
30. Rice, P., Longden, I., and Bleasby, A. (2000) EMBOSS: the European Molecular Biology Open Software Suite, *Trends Genet. 16*, (6), 276–277.
31. Gasteiger, E., Hoogland, C., Gattiker, A., Duvaud, S., Wilkins, M. R., Appel, R. D., and Bairoch, A. (2005) Protein Identification and Analysis Tools on the ExPASy Server, in *The Proteomics Protocols Handbook* (Walker, J. M., Ed.) pp 571–607, Humana Press, Totowa, NJ.
32. Cornette, J. L., Cease, K. B., Margalit, H., Spouge, J. L., Berzofsky, J. A., and DeLisi, C. (1987) Hydrophobicity scales and computational techniques for detecting amphipathic structures in proteins, *J. Mol. Biol. 195*, (3), 659–685.
33. Maiti, R., Van Domselaar, G. H., Zhang, H., and Wishart, D. S. (2004) SuperPose: a simple server for sophisticated structural superposition, *Nucleic Acids Res. 32*, (Web Server issue), W590–W594.
34. Dosztanyi, Z., Csizmok, V., Tompa, P., and Simon, I. (2005) IUPred: web server for the prediction of intrinsically unstructured regions of proteins based on estimated energy content, *Bioinformatics 21*, (16), 3433–3434.
35. Lambert, C., Leonard, N., De Bolle, X., and Depiereux, E. (2002) ESyPred3D: prediction of proteins 3D structures, *Bioinformatics 18*, (9), 1250–1256.
36. Comeau, S. R., Gatchell, D. W., Vajda, S., and Camacho, C. J. (2004) ClusPro: a fully automated algorithm for protein-protein docking, *Nucleic Acids Res. 32*, (Web Server issue), W96–W99.
37. Comeau, S. R., Gatchell, D. W., Vajda, S., and Camacho, C. J. (2004) ClusPro: an automated docking and discrimination method for the prediction of protein complexes, *Bioinformatics 20*, (1), 45–50.
38. Sayle, R. A., and Milner-White, E. J. (1995) RASMOL: biomolecular graphics for all, *Trends Biochem. Sci. 20*, (9), 374.
39. Humphrey, W., Dalke, A., and Schulten, K. (1996) VMD: visual molecular dynamics, *J. Mol. Graphics Modell. 14*, (1), 27–28; 33–38.